Challenges of Polarimetric Weather Radar Calibration

Rich Ice

Richard L. Ice, A. K. Heck, J. G. Cunningham and W. D. Zittel

WSR-88D Radar Operations Center, Norman, Oklahoma, United States of America
(15 July 2014)

Abstract

The United States' Next Generation Weather Radar (NEXRAD) program has deployed a polarimetric upgrade to the WSR-88D network radars. This modification provides new base variables to the operational community and has opened exciting new possibilities for improved forecasts and warnings. One variable in particular, differential reflectivity (Z_{DR}), is critically important to improved precipitation estimates and hydrometeor classification. However, the quality of the differential reflectivity estimate is highly dependent on the removal of biases induced by the radar system hardware. These biases must be measured to an uncertainty of 0.1 dB in order to obtain maximum benefit from the polarimetric data and meteorological algorithms.

This paper will review the engineering challenges being faced in our efforts to further improve the calibration of the WSR-88D to the required level of accuracy focusing on the use of microwave hardware measurements and solar scans. We also offer some rules, or guides, to foster successful calibration system design and implementation.

1 Introduction

A joint US government and contractor team completed deployment of the polarimetric upgrade to the United States' Next Generation Doppler weather radar network (NEXRAD) in the Spring of 2013. The dual polarization version of the US network had been under consideration since the 1980's, and at that time researchers were aware of the potential measurement accuracy requirements (Sirmans, 1984). Since deployment activities began, scientists and engineers at the ROC have been monitoring network performance, estimating differential reflectivity bias and assisting site personnel as problems have been discovered. This paper describes efforts at the ROC to develop methods for estimating the bias errors and will address potential improvements to the calibration process.

The concept of measuring radar returns from precipitation at orthogonal polarizations dates back to the 1970's. At that time, researchers were already considering the effects of errors on the usefulness of polarimetric data. Seliga and Bringi (1976) described the sensitivity of rain rate distribution parameters to the radar measurement error. They provided uncertainty estimates related to Z_{DR} measurement errors of 0.2 dB and 0.5 dB, noting that they felt these error bounds were reasonable since Z_{DR} is a differential measurement. With this study, Seliga and Bringi established the initial range of requirements for Z_{DR} uncertainty. As was determined, the desired accuracy evolved into a need for uncertainties of 0.1 dB or less. Meeting this need has been quite a challenge for the design and implementation of operational systems.

Accurate calibration of the new hardware is essential for the NEXRAD community to gain maximum benefit from use of the new polarimetric variables. The most critical parameter is differential reflectivity (Z_{DR}), which is derived from the ratio of return powers in the horizontal and vertical channels. In order to retrieve the intrinsic, or true, measure of Z_{DR}, the contribution of the radar hardware itself to this power ratio must be removed. This contribution, or bias, originates from several components of the radar. There can be an imbalance in the transmitted powers, i.e. the horizontal and vertical components of the divided transmitter power may not be equal. The gains of the antenna in the horizontal and vertical paths may not be exactly the same, and finally, the two receiver channels will likely not exhibit the same overall gain and will generate different levels of electronic noise. The receiver channel gain imbalance is a particularly challenging aspect since the performance of the two channels can vary

considerably over time, as a function of temperature for example. Measuring the receiver bias once with a high degree of precision is insufficient. The receivers must be tested on a frequent basis in order to maintain system calibration.

Accurately determining the biases related to the horizontal and vertical channels in all these subsystems constitutes the process of differential reflectivity calibration. This paper reviews the Z_{DR} calibration methods provided in the initial design and development of the upgrade and provides descriptions and status of development for the current projects underway at the WSR-88D Radar Operations Center (ROC), the National Center for Atmospheric Research (NCAR) and the National Severe Storms Laboratory (NSSL). These partners are actively pursuing new methods of monitoring the state of Z_{DR} calibration in the network, and are developing modifications to the calibration process in order to provide the necessary accuracy. ROC and NSSL teams have developed methods for estimating errors using external targets such as rain, dry snow and Bragg scatter (Zittel, 2014; Hoban, 2014; Cunningham, 2013). The ROC and NCAR are implementing an external method based on the use of cross polarization power returned from ground clutter (Ice, 2013; Meymaris, 2013; Hubbert, 2003, 2012).

This paper further reviews the benefits of associated with maintaining a good calibration state in the WSR-88D. These challenges can be met with a combination of engineering calibration improvements and external target monitoring.

2 Motivation – Why Calibrate?

As mentioned above, researchers recognized early that accurate measurements of the differential power would be critical to the success of polarimetric weather radar. Of course, requirements for accurate measurements are not exclusive to polarimetric radars. For non-polarimetric radars, precipitation estimation algorithms were primarily based on reflectivity. The traditional requirement for the uncertainty in the reflectivity estimate (dBz; Smith, 2010) is 1.0 dBz (Ice, 2005; Sirmans, 1992). This is the level of accuracy needed to obtain acceptable rainfall rate accuracy. While the original WSR-88D hardware and software was believed to be capable of calibration to this requirement, it proved difficult to achieve in practice in the early days of NEXRAD (Ice, 2005). In fact, upon the initial deployment of the network in the early 1990's, the government did not have a practical method for calibrating the hardware.

The Engineering Branch of the ROC developed a comprehensive method for reflectivity calibration, but problems remained until a network monitoring capability was established. This capability was based on a software tool that compared the reflectivities from adjacent radars with the objective of identifying specific radars that required attention when their estimates on common volumes of precipitation were in disagreement with their neighbors (Gourley, 2003). Reflectivity calibration accuracy and stability was not consistently achieved until this monitoring capability was in place and several issues with antenna gain measurement were resolved (Ice, 2005).

With the polarimetric capability, a new Quantitative Precipitation Estimation (QPE) algorithm is being deployed (Berkowitz, 2013). This algorithm relies on the new polarimetric variables in order to provide precipitation estimates with less error than the legacy algorithm which used reflectivity alone. The QPE method consists of three parts: (1) Hydrometeor Classification Algorithm (HCA), (2) Melting Layer Detection Algorithm (MLDA), and (3) the QPE algorithm itself. The outputs of the HCA and MLDA are critical inputs to the QPE. All three use reflectivity, differential reflectivity, cross correlation coefficient, and specific differential phase as inputs.

In order for the QPE, or for any rain rate estimator using differential reflectivity, to perform substantially better than the legacy estimator, the differential reflectivity must be estimated to within an error limit of 0.1 to 0.2 dB (Zrnić, 2010; Ryzhkov; 2005, Brunkow; 2000; Bringi, 1983). It is interesting to note that a range of 0.1 to 0.3 dB was considered achievable with sufficient numbers of samples processed (Bringi, 1983). For light to moderate rain, the 0.1 dB accuracy must be achieved to maintain rain rate error estimates at around 10%. For heavier rain, the accuracy can be relaxed to 0.2 dB. If the error in calibration is greater than about 0.3 dB, then the polarimetric precipitation estimators do not perform substantially better than non-polarimetric algorithms.

The primary source of error in the Z_{DR} estimate is the uncertainty in the measurement of the system bias, or the contribution to the overall power ratio coming from the radar hardware. The accurate measurement of this value, the system bias, has been the focus of much attention over the past ten years (Zrnić, 2006).

Various methods for determining the system bias have been studied and used in the research community. The common practice is to obtain careful measurements of the differences between the two polarization channels (H and V) for the transmitter, receiver, and antenna. However, even with careful measurements using well calibrated instruments, the overall uncertainty of the bias has historically been greater than the required tolerance. Most research radars have been calibrated using a method that rotates the radar antenna through 360 degrees while pointing it in a vertical position in the presence of light rain (Gorgucci, 1999). This calibration method takes advantage of the azimuthal symmetry resulting from the rain drops appearing spherical from below (Bringi and Chandra, 2001). This symmetry of the scatterers results in an expected mean value of zero for Z_{DR} in the resolution volume. A non-zero mean value of the Z_{DR} estimate obtained in this manner would be equivalent to the radar system bias.

To date the vertical pointing method has been considered the best external means of obtaining the system bias. During the development of the prototype upgrade for NEXRAD, the KOUN radar was calibrated using careful engineering measurements (Zrnić, 2006). The program did not develop an external method although the use of precipitation at angles other than vertical were explored (Ryzhkov, 2005). The production WSR-88D polarimetric upgrade was delivered with a sophisticated calibration capability based on hardware measurements combined with solar scans (Balaji, 2012). The next section presents the baseline WSR-88D engineering calibration method.

3 The WSR-88D Baseline Method

The WSR-88D in its baseline configuration does not have the capability to point vertically, so the classic method was not available for the production NEXRAD polarimetric upgrade without modifications to the antenna pedestal hardware. Also, it was undesirable to take the radars offline during precipitation events in order to perform calibration vertical pointing scans. Much of the focus of the design and development of the production hardware focused on calibration and the contractor, Baron Services Inc., provided the necessary hardware components and procedures for conducting what came to be known as an “engineering method”. This method is currently employed to obtain the bias components for the transmitted signal, the receiver channels, and the antenna.

Figure 1 is a simplified block diagram of the WSR-88D showing the three major subsytems relevant to Z_{DR} calibration (transmitter, receiver, antenna). The bias elements that contribute to the calibration problem are the receiver channel bias (RCB), the transmitter bias (TXB), and the antenna bias, designated as sun measurement bias (SMB). The antenna bias is designated as sun measurement bias because solar scans are used for this measurement. Note that the three subsystems come together at a common point known as the calibration reference plane. This is established as the dividing point for separating out the three distinct components of the overall system bias. At this point, waveguide couplers are provided that allow insertion of test signals (for receiver bias measurements) and for extracting samples of the signals within the waveguide (for transmitter power measurements).

The baseline hardware suite contains all of the necessary components for generating the receiver test signals and for extracting and processing the transmitter power samples from both channels. However, the hardware components that establish and maintain the bias measurements can introduce errors, and these must be measured. Calibration is then the process of characterizing the built-in-test equipment by measuring the bias introduced by the receiver test signals (test signal bias) and the transmitter power measurement hardware (power sense bias) and obtaining the antenna bias from solar scans. These three measurements are recorded and used to establish an initial state of calibration. Once the initial state of calibration is established, these parameters are used to maintain the calibration state through periodic measurements.

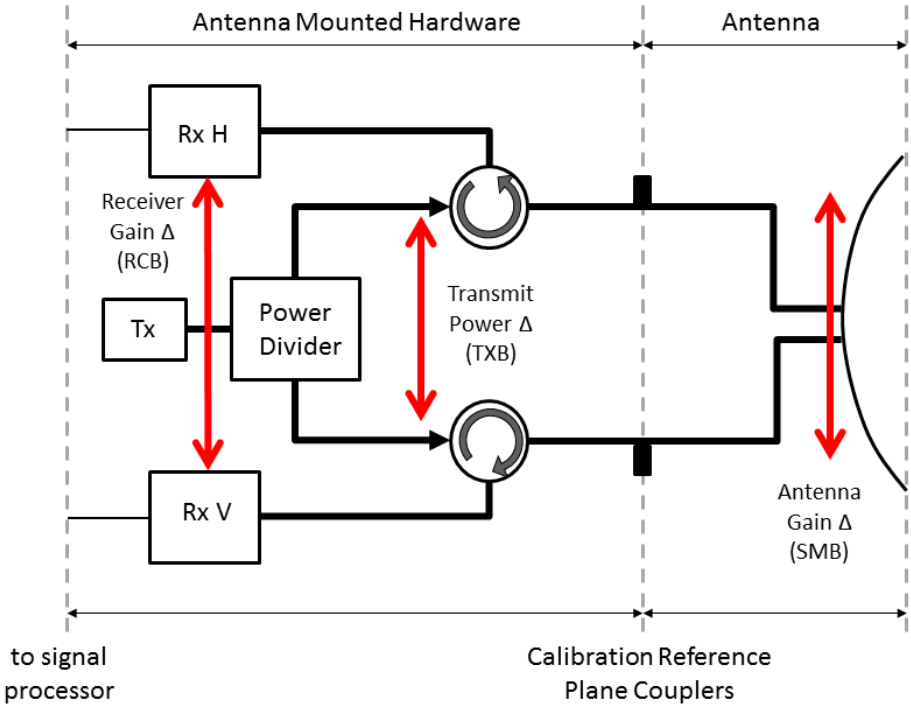

Figure 1: Calibration Subsystems Basic Diagram

Calibration consists of determining the values of the three elemental biases described above, and combining them. For the WSR-88D the following equation applies:

$$Z_{DR}\ \text{offset} = 2^{*}\ \text{SMB} + \text{RCB} + \text{TXB} \qquad (1)$$

SMB is included with a factor of 2 because it is the one-way measurement of antenna bias, and the antenna is a common component of the signal transmission and reception processes.

3.1 The Calibration Reference Plane Couplers

As mentioned, the calibration process relies heavily on the use of microwave couplers for injecting receiver test signals and for measuring the transmitter power balance. The designed insertion loss of the couplers is 30 dB, meaning that the signals measured at the output port are 30 dB lower in power than the level existing within the waveguide. The actual value of the loss for any particular coupler at the radar unit's operating frequency must be known to a high degree of accuracy. Moreover, the value depends on the direction of coupling. The so called forward coupling factor, which is associated with power measurements, is different from the reverse coupling factor that is part of test signal injection.

The coupling factors are measured by the hardware manufacturer, using a vector network analyzer calibrated with the Through-Reflect-Line (TRL) method. The four parameters supplied for the power sense (forward) and signal injection (reverse) coupling factors are: R293, H channel reverse coupling; R294, V channel reverse coupling; R295, H channel forward coupling; and R296, V channel forward coupling. The "R" designators are the terms used in the WSR-88D software.

There has been considerable debate over the accuracy with which the coupling factors can be measured. Engineers at NCAR studied the problem as part of a task that examined the limitations of hardware calibrations for polarimetric measurements (Hubbert, 2008, 2007b). The NCAR study concluded that the cumulative errors of coupling factor measurement error along with the uncertainty associated with disconnecting test cables for the various measurements would yield an overall bias uncertainty for these engineering type calibrations of at least 0.25 dB. ROC engineers analyzed the coupling factor data supplied by the manufacturer. Figure 2 is a series of plots of the coupling factors for one set of H and V couplers, with the factors presented over the radar frequency range of 2700 to 3000 MHz. The manufacturer provided data in 5 MHz increments.

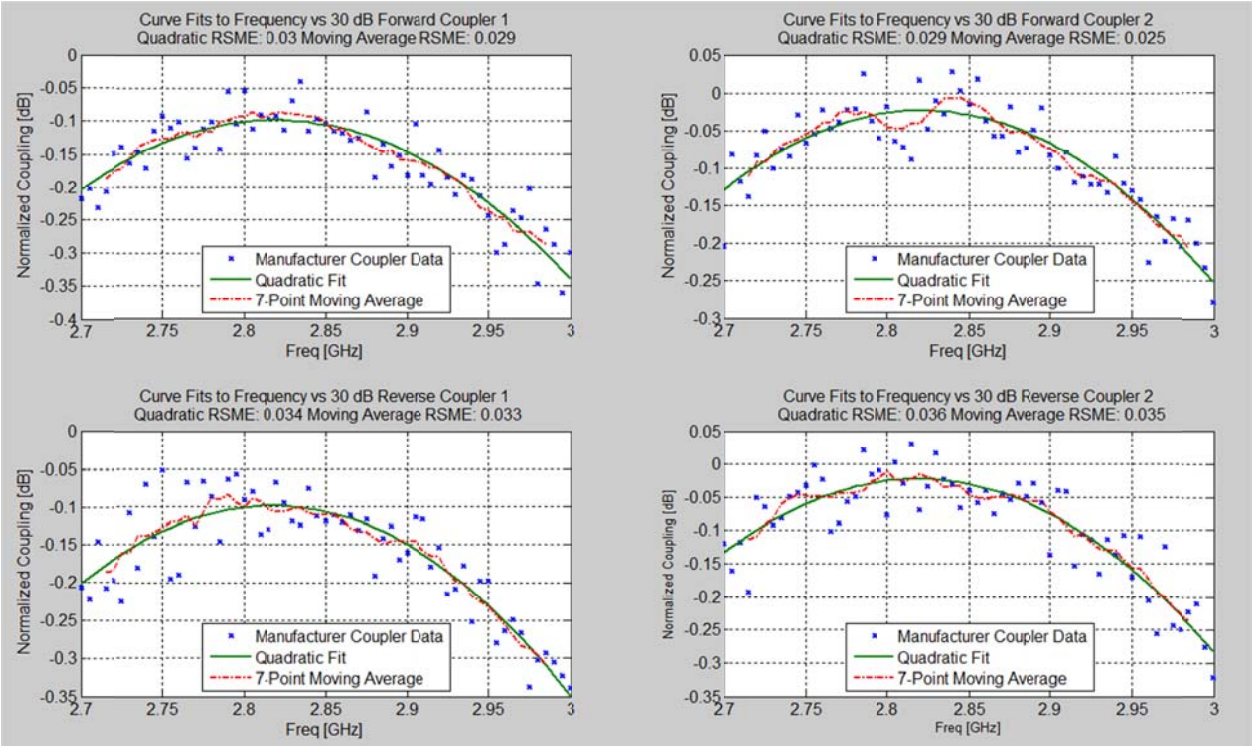

Figure 2: 30 dB Coupler Data

The notable feature of this data set is the considerable spread of the values as the frequency is incremented over the range. At some frequencies, the value changes by up to 0.1 dB from one frequency to the next.

3.2 Obtaining the Test Signal and Power Sense Bias Parameters

The biases from the test signal and power sense functions are obtained off-line when the technicians perform calibration. These biases are measured during a process where the technician crosses the connections to the calibration reference plane couplers, then runs automatic tests that record the output of the H channel receiver for both receiver bias tests and the transmitter power monitoring. Then the technicians return the coupler connections to the normal (uncrossed, or "straight") configuration and run the tests again. Figure 3 illustrates the process for the test signal bias. As seen in the diagram and accompanying equations, the difference in the H receiver outputs between the crossed and straight configurations yields the bias between the H and V test signals that exists at the input to the receiver. The value for the test signal bias (designated as R297 in the WSR-88D software), is stored for use in the active determination of receiver bias described below. The calibration process to obtain the power sense bias is similar. The value for power sense bias, necessary for transmitter bias measurements, is stored in the WSR-88D software and is designated as R298.

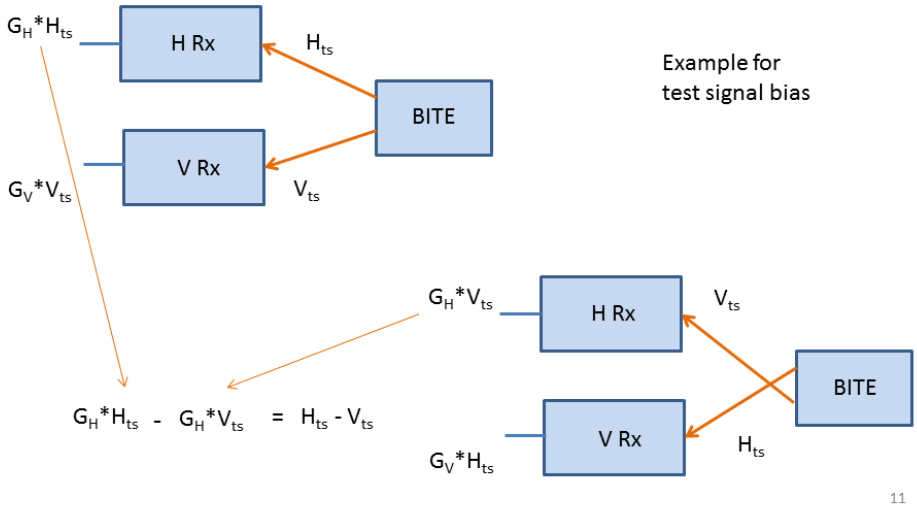

Figure 3: Example of Method for Obtaining Test Signal Bias (R297)

This is a theoretically simple and elegant method for obtaining the test bias numbers. However, in practice, results of this process can be inconsistent. For this reason, the system procedures require that several measurements be made and a consistency check is done before final results are accepted.

The polarimetric hardware is mounted on the elevation arms of the antenna pedestal assembly. The advantage of this configuration is that the low noise amplifiers are located very near the antenna port, thus improving sensitivity. Also, since the power divider function is on the antenna, the H and V waveguide paths to the feed assembly are shortened, thus reducing effects of differing path lengths on overall system initial phase and perhaps allowing the system phase to be more stable over time. The disadvantage to this configuration is that maintenance can be difficult.

In order to perform the crossed and straight calibration process, the technicians must stand on a ladder and reach behind some of the waveguide components. Figure 4 shows a view of the RF microwave components, or the RF Pallet from the floor of the dome area with the ladder in place. The small inset photos of Figure 4 show the connectors and Heliax cables that are crossed for the tests. The connectors are of a snap-on variety that were selected to allow consistent results from multiple connections.

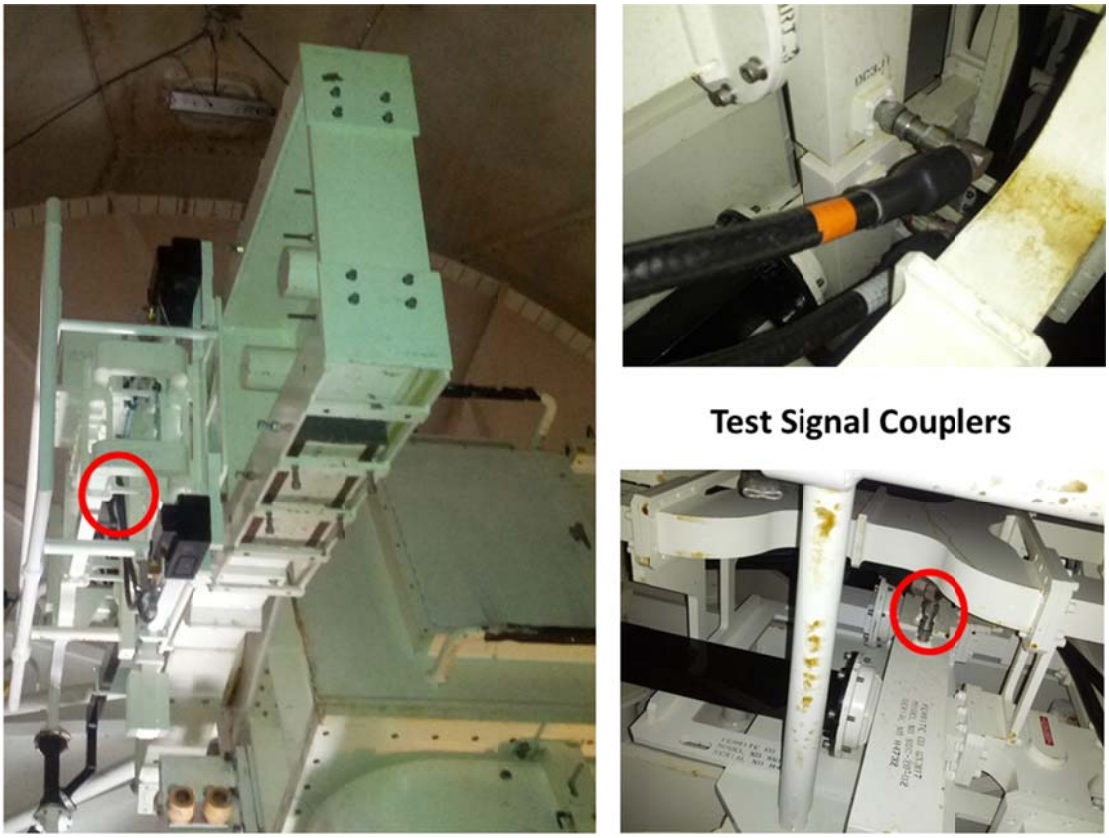

Figure 4: Test Signal Couplers

3.3 Receiver Bias Measurement

The receiver bias measurement is demonstrated in Figure 5, which shows a simplification of the use of the test signal. Equal power continuous wave (CW) signals from the built-in test equipment (BITE) are inserted into the front end of the receiver channels using the couplers at the calibration reference plane. The desired outcome is that the test signals are equal in power and thus any non-zero ratio of powers obtained at the signal processor would be the result of the bias, or imbalance, between the H and V receiver. In reality, the powers in the two test signals are not exactly equal, and the total path losses from the BITE equipment to the inputs to the receivers are not equal. These differences, or the test signal bias, is the elemental bias measured in the off line process described in Section 3.2. The test signal bias is indicated by the red arrow in Figure 5.

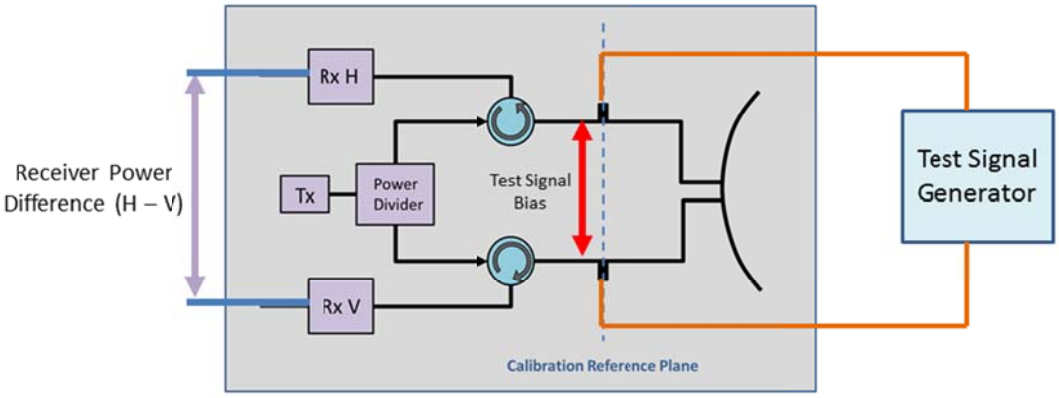

Figure 5: Receiver Bias Measurement

The test signal bias parameter (designated R297 in the WSR-88D software) is then used, along with the appropriate coupler losses, to compute the receiver channel bias per the following equation:

$$RCB = (Hpow - Vpow) - R297 - (R293 - R294) \quad (2)$$

where Hpow and Vpow are the signal powers as measured by the digital receiver. Also note that the 30 dB coupler reverse losses for both H and V channels are included (R293 and R294).

3.4 Sun Measurement Bias

The antenna bias is obtained from a relatively straightforward scan of the sun, relying on the assumption that the sun is un-polarized (Figure 6). This "sun bias" obtained from the scan is the ratio of noise powers between the two channels where the signal source is the noise power of the sun itself. However, the actual bias contribution from the antenna component can only be inferred from the results of the solar scan because the ratio of the noise powers obtained at the signal processor includes not only the bias from the antenna, but contains the bias from the receiver, and this must be removed. In the calibration process, the result of subtracting the receiver bias from the sun bias measurement is called "reflector bias". Obviously, an error in measuring the receiver bias creates an error in the reflector bias.

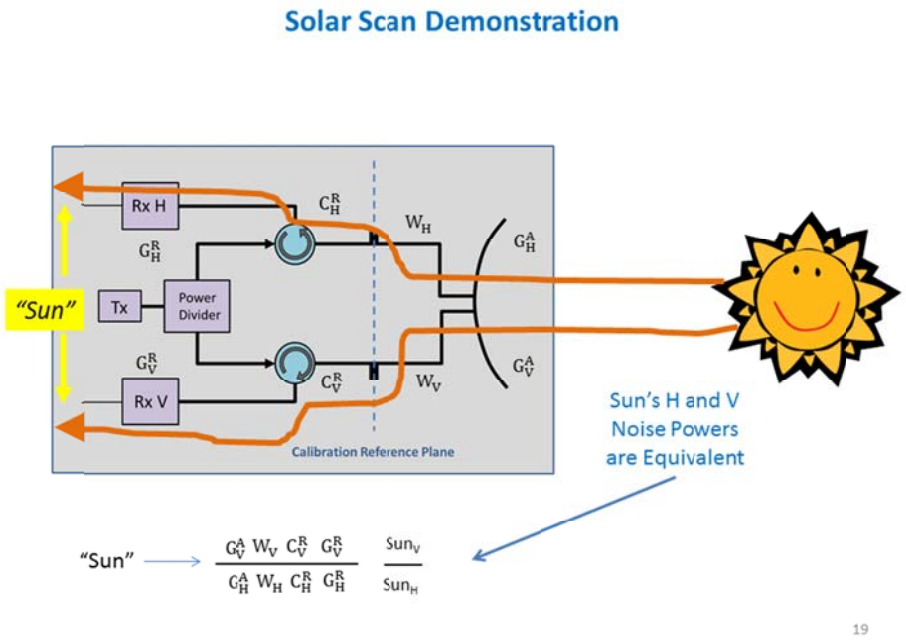

Figure 6: Solar Scan Concept Demonstration

The sun measurement bias is computed using the following equation:

$$SMB = (Hsun - Vsun) - RCB \quad (3)$$

where Hsun and Vsun are the noise powers as measured by the H and V digital receiver channels at the time of the solar scan. Also note that SMB is dependent on the value of RCB at the time of the solar scan. So a receiver bias measurement is always done in conjunction with a solar scan.

The method of scanning the solar disk is important in order to obtain good results. The baseline system delivered by the dual polarization contractors was a modification of the legacy WSR-88D method. The legacy method consists of two operations, or sub-tests. Subtest 1 scans the antenna main beam 3 degrees about the expected location of the sun in azimuth and elevation while the sun passes through the antenna main lobe due to the motion of the earth. Once the noise powers of the solar signal have been collected, the software creates a plot of power as a function of angle, both in azimuth and elevation, where the angles are those reported by the pedestal control electronics. The software then fits a parabolic curve to the power data, finds the peak, and compares that peak to the elevation and azimuth of the expected position of the sun at the associated time, based on a precise astronomical model. The difference in the position of the measured peak and the expected position of the sun is the error in antenna positioning due to misalignment of the antenna and the control electronics. These difference correction factors are presented to the radar operator or technician and can be used to refine the accuracy of antenna positioning. Figure 7 is a sample of a plot presented to the technician for quality control purposes.

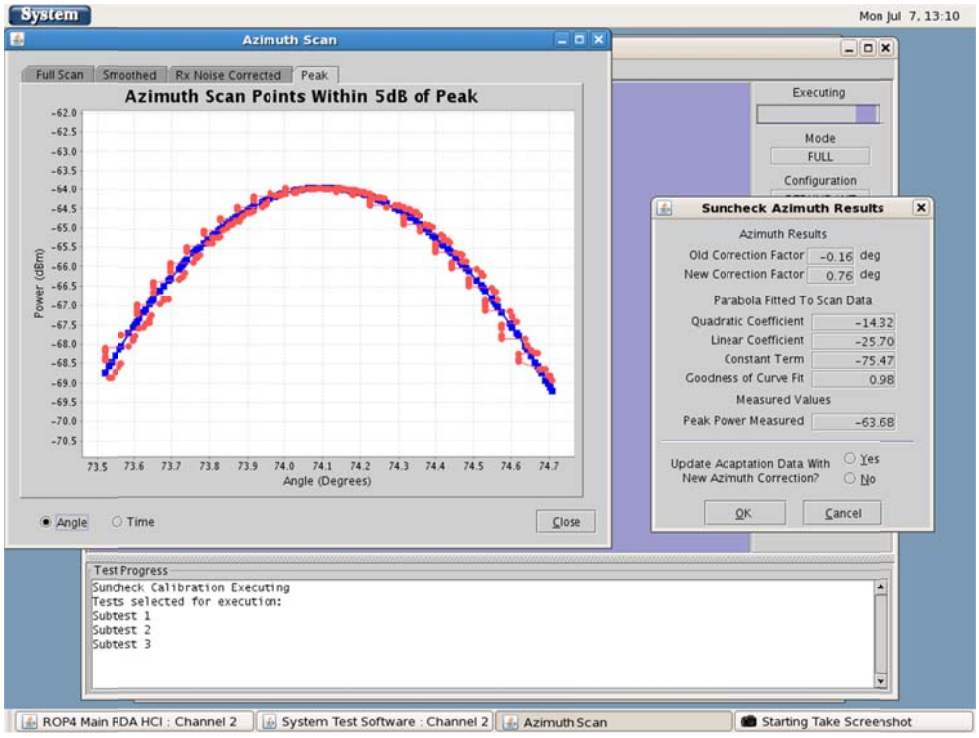

Figure 7: Display of Azimuth Solar Scan Fit to Sun Noise Power

Figure 7 shows the sun's noise power during the scan as a function of azimuth angle, and depicts the expected parabolic curve resulting from the movement of the antenna main beam across the solar disk. The peak of the fitted parabola can then be compared to the expected peak derived from the astronomical model. The display shows the recommended azimuth correction factor as well as the goodness of fit for the parabola. Technicians are instructed to only accept results with sufficient goodness of fit, 0.98 or better.

Sub-test 2 is the antenna gain measurement. The measured noise power of the sun is compared to the expected noise power calculated from data supplied by a solar observatory, typically the 10.7 cm flux from the Penticton observatory (Free, 2007). Sub-test 3 is a new function supporting the polarimetric upgrade. This test computes the ratio of the H and V powers at the peaks in order to obtain the antenna bias. Issues with the solar scans, especially related to errors in antenna positioning and noise contamination due to interference, have been a source of significant errors in the differential reflectivity process.

3.5 Transmitter Bias Measurement

In an ideal radar, the transmitted H and V powers would always be equal. This could be achieved in practice by using a perfect splitter to divide the transmitter signal in to equal parts, and then by carefully matching the waveguide and circulator systems up to the antenna. In the case of the WSR-88D polarimetric upgrade, a more complex method of dividing the transmitter power is employed. The contractor delivered a capability to establish any ratio of transmitted power between the H and V channels through use of a variable phase power divider. This divider can continuously deliver ratios of H to V power under computer control ranging from all H to all V and any ratio in between. In normal operations, the power ratio is set such that the H and V transmitter powers are equal. Because the ratio is variable, and since it is never possible to perfectly match components, the H and V powers must be measured.

The transmitter power imbalance is measured in a similar manner, using the couplers at the calibration reference plane and the BITE system. Figure 8 illustrates the process. A unique feature of the transmitter power measurement is that the measurement device is the receiver signal processor itself, in particular the H receiver channel. The V and

H powers have to be measured separately due to this and the fact that there is only one hardware delay line available in the BITE system. The sampled transmitter signals must be delayed because the receivers are blanked by the TR Limiter component during transmission. The BITE system provides the necessary switching and routing components for alternatively connecting the H and V couplers and routing the samples to the H receiver.

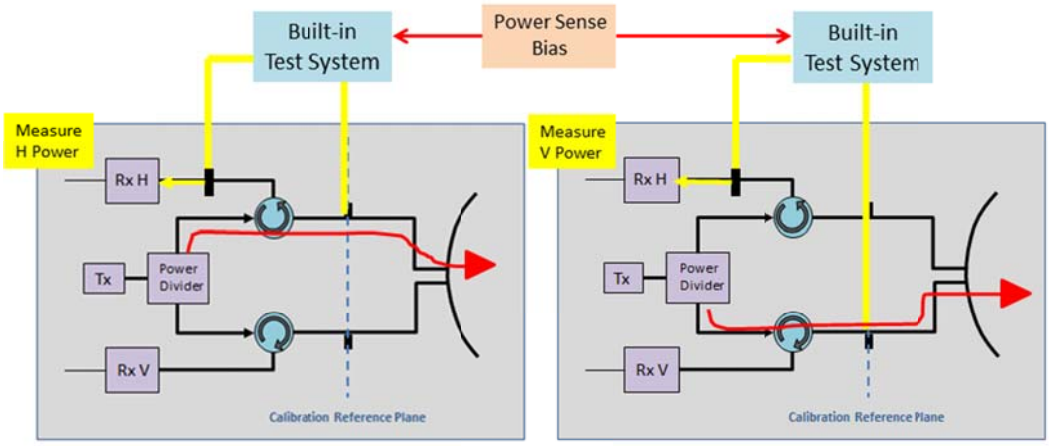

Figure 8: Transmitter Power Bias Measurement

The BITE system introduces an error into the measurement of the ratio of the H and V samples, and this must be measured at the time of calibration. The power sense bias component is indicated by a function in Figure 7. The power sense bias is the value stored in adaptation data that was generated by the off-line process described in Section 3.2 (R298). It is used to correct the power measurements when they are made periodically during operations.

The transmit bias (TXB) is computed in the WSR-88D using the following equation:

$$TXB = (Hps - Vps) - R298 - (R295 - R296) \quad (4)$$

where Hps and Vps are the horizontal and vertical powers as measured by the digital receiver during the respective power sense operations. Again, R298 is the bias of the power sensing equipment and R295 and R296 are the H and V forward coupling factors.

3.6 Continuous Calibration Process

During operations, the system Z_{DR} is constantly measured and updated using the three calibration parameters discussed here. The correction factor is updated for every radar volume scan. At the end of every volume scan, the BITE injects test signals into the receiver channels in order to update the receiver bias component of the overall system bias. The BITE also measures the noise power in each channel at the top elevation position which is corrected for lower elevations using a preset table. Also, the receiver noise figure is measured using a local noise source calibrated to a traceable standard. Periodically, typically every eight hours, the transmitter power balance is updated. The transmitter power ratio is not measured every volume because the process takes about two minutes and this would cause unacceptable delays in the volume update rate. The antenna bias measurement is done less frequently, on a monthly scale. The Z_{DR} offset, which corrects the raw differential reflectivity, is updated each volume scan using the bias equation (1), which is repeated here for reference.

$$Z_{DR}\ \text{offset} = 2^* \text{SMB} + \text{RCB} + \text{TXB}$$

The ROC can track changes in the calibration parameter over time using a network tool. Figure 9 is a sample of the Z_{DR} offset, called "Sys ZDR Calib Constant" in this plot. The data is for the North Platte, Nebraska WSR-88D and shows how the calibration parameter changes over a period covering 20 days in June and July, 2014.

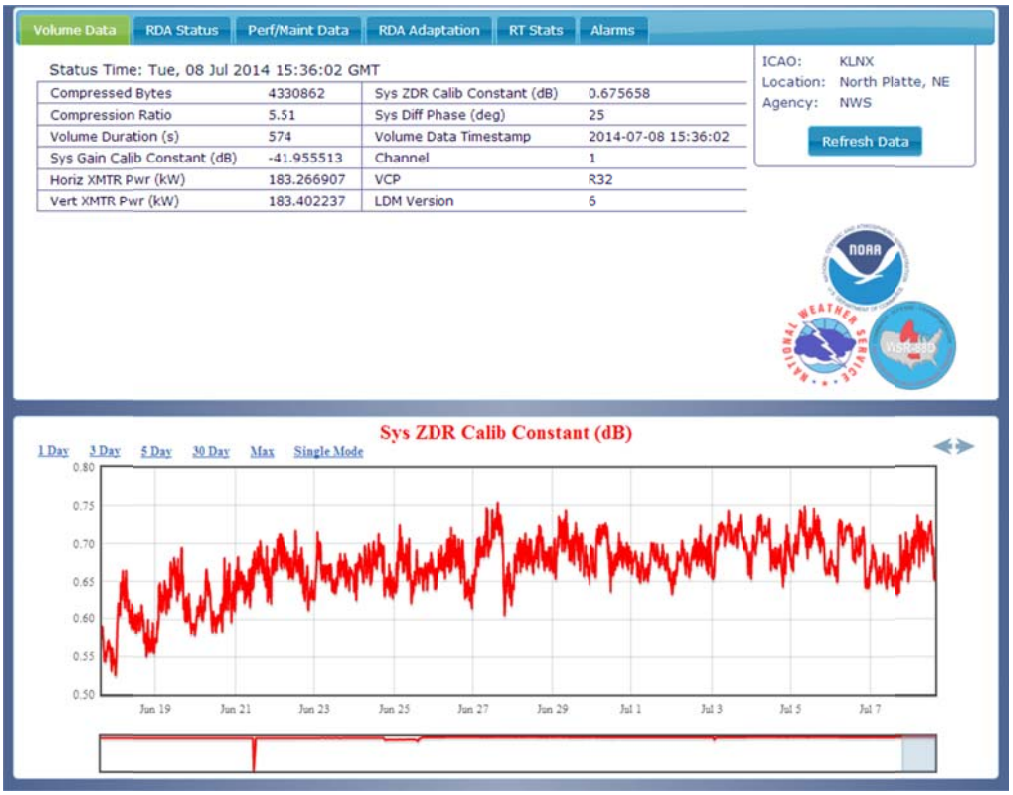

Figure 9: Differential Reflectivity Calibration Parameter Tracking

4 Observed System Performance

The development teams and the government spent considerable effort reviewing, analyzing, and testing the hardware and software systems with respect to calibration. However, due to the challenging nature of verifying the Z_{DR} bias externally, there was no formal test of the calibration capability. The contractor was required to verify compliance with the 0.1 dB accuracy specification by use of analysis. Baron Services engineers conducted a theoretical analysis which included some hardware measurements. This analysis demonstrated that the delivered design was capable of meeting the requirement (Baron Services, 2011) and the government accepted the results (Saxion, 2012).

Engineers at Baron Services, working with data obtained shortly after initial installations, analyzed the Z_{DR} bias measurements and concluded that the system was performing as designed (Balaji, 2012). Balaji's analysis showed the system bias values for ten radars obtained every volume for 1600 trials. The resulting histograms and time series plots showed the stability of the process was quite good, although there was a range of Z_{DR} calibration offset values between the sites. One site exhibited a system bias of less than -1.3 dB, which was greater than the average of the other sites and could indicate an error in calibration.

ROC engineers and the joint Data Quality Team also monitored the hardware performance on a regular basis, during the development as well as the early deployment stages (Saxion, 2012). Initial results were encouraging, showing very good stability in the hardware over time and early indications were that the test radar calibration was adequate, as well as it could be assessed with the emerging external verification methods. These methods were

based on observing expected values of Z_{DR} under certain weather conditions such as light precipitation. These observations were based on expected values of differential reflectivity resulting from many years of research into Z – ZDR relationships for various types of precipitation (Cao, 2008; Bringi, 1991; Illingworth, 1989; Bringi, 1983).

Now that the network upgrade is complete, and the ROC has implemented monitoring processes, it has become evident that the calibration process is not producing consistent results. The ROC team has observed that up to 40% of the sites have estimated system bias errors of greater than 0.2 dB (Cunningham, 2013). This observation is based on the use of the weather comparison method mentioned above as well as a new method based on the use of the daily sun spikes seen each morning and evening (Holleman, 2010; Huuskonen; 2007). In addition to these methods, the ROC is developing another external target method based on Bragg scatter (Hoban, 2014; Melnikov, 2013a; 2011). This latter method is based on the assumption that the Bragg scatter is also polarization neutral like the solar radiation noise power.

Error of greater than 0.2 dB, as estimated by these methods, can affect the polarimetric Quantitative Precipitation Estimator (QPE), lowering rain rate estimate accuracy. For errors in the 0.3 to 0.4 dB range, the accuracy approaches that of the non-polarimetric estimators. However, substantial benefits are achieved in hydrometeor classification and identification of warning indicators such as Z_{DR} columns and debris signatures, even for errors greater than these.

The ROC Hotline provides assistance to sites that may be incorrectly calibrated. The Hotline provides calibration assistance upon request when the operational community observes issues with Z_{DR} estimates or precipitation estimator outputs. The ROC Hotline also monitors performance of the sites and can offer assistance when unusually poor performance is noted.

The engineering teams also can monitor the statistics of the three critical calibration parameters. This data may prove useful for improving technical manual procedures and test equipment in the field. Figure 10 is a histogram of the reflector bias (SMB, parameter a31) for the WSR-88D fleet as of May 20, 2014. While the majority of the sites reported reflector bias values of near zero, there are many that have unexpectedly large bias values. Errors in the reflector bias can exacerbate problems with overall system calibration because this bias is counted twice in the calibration correction equations because it enters into both the transmit and receive components of the Z_{DR} estimate.

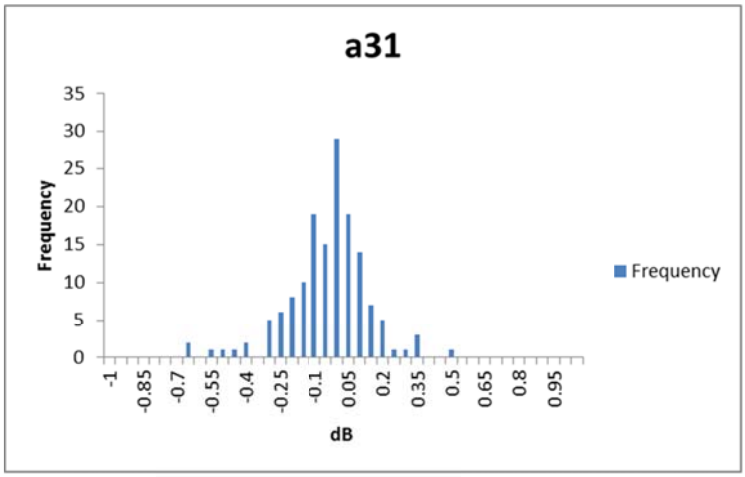

Figure 10: Histogram of WSR-88D SMB across the WSR-88D Fleet (May 20, 2014)

Figures 11 and 12 show similar histograms for the power sense and test signal bias for the same 146 sites. The ROC team plans to continue investigating the field performance and the effects the variance of these parameters has on the calibration accuracy.

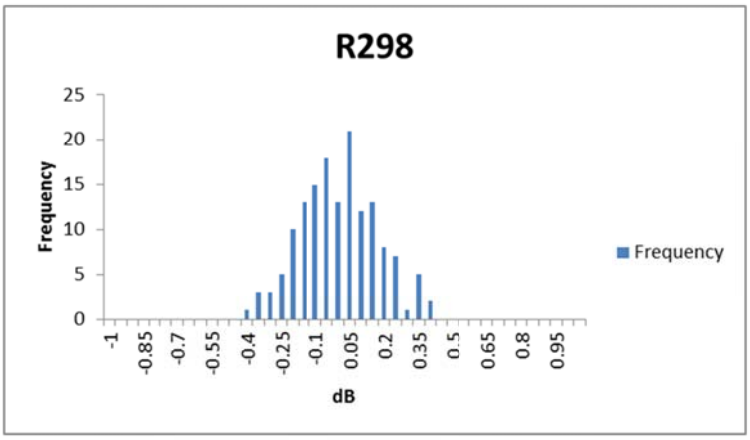

Figure 11: Histogram of Transmit Power Sense Bias across the WSR-88D Fleet (May 20, 2014)

The ROC's capability for monitoring system performance includes many parameters relevant to calibration. Figure 13 is a plot of the H and V transmitter powers for the North Platte radar over the same period as the data in Figure 9. It shows how the H and V powers, in kW as measured by the built in test equipment, track each other for a 20-day period. Note that while the absolute powers vary, indicating fluctuating transmitter powers, the ratio of the powers of the H and V transmission signals remain constant.

While the ROC teams are developing external verification methods through the use of weather signals and the sun, they have also been implementing and testing an alternate method based on measuring the power returned from ground clutter in the cross polarization receiver channels. The next section provides a description and status of this independent method.

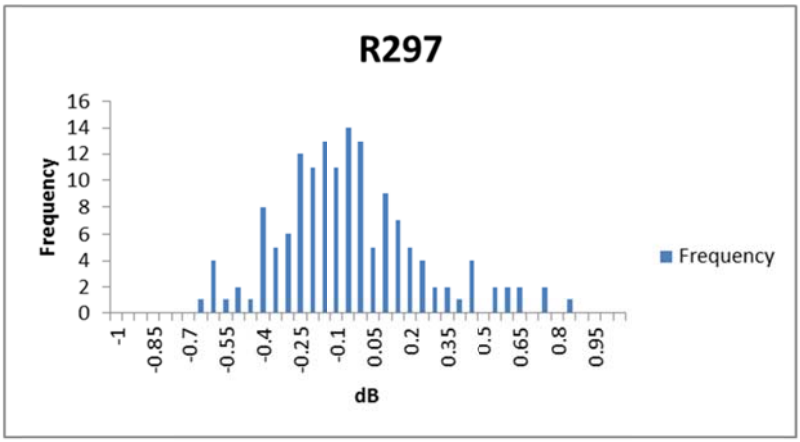

Figure 12: Histogram of Test Signal Bias across the WSR-88D Fleet (May 20, 2014)

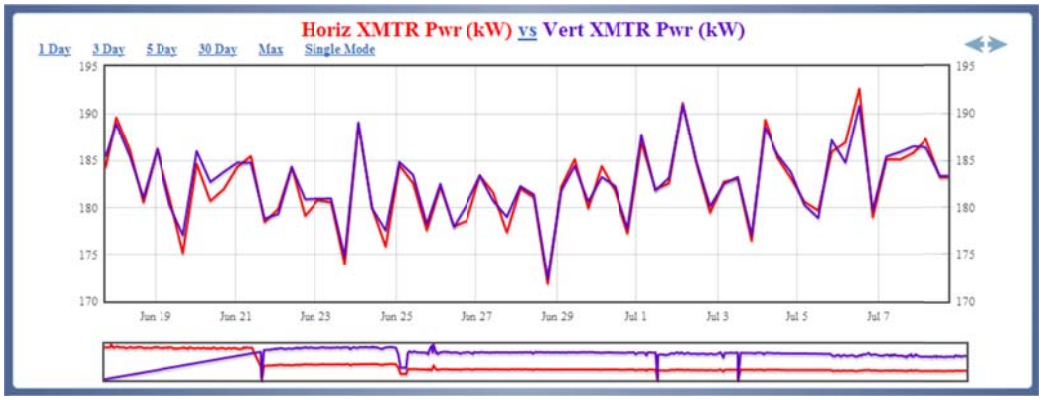

Figure 13: H and V Transmit Powers for the North Platte, NE, WSR-88D, June 18 to July 8, 2014

Likewise, the system noise is measured at the end of each volume scan. Figure 14 shows the H and V channel IF noise powers over the same 20-day period. Note the diurnal variation in the absolute noise powers. This is most likely due to temperature variations. While the system exhibits daily variations, the relation between the H and V noise is relatively constant. There are a couple of exceptions in this data set. Early in the period it appears that the vertical noise power is about 0.1 dB greater than the horizontal power for a short period.

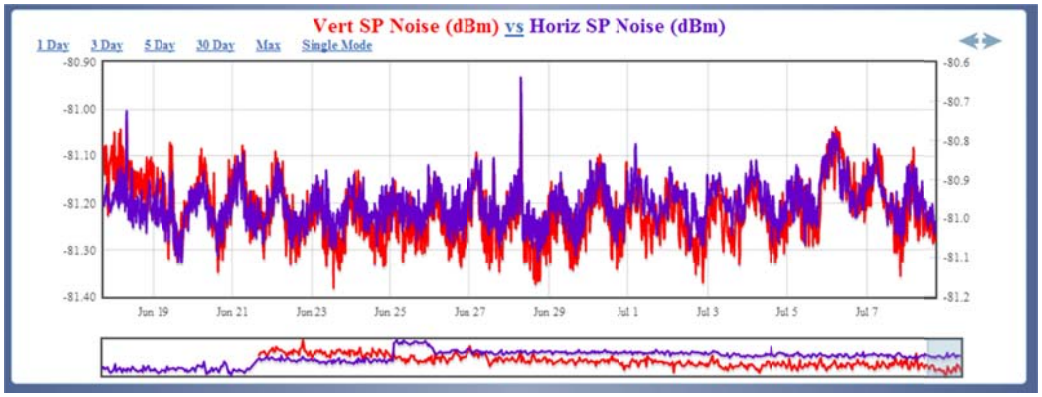

Figure 14: IF Channel Noise Measurements (H and V) for the North Platte, NE, WSR-88D, June 18 to July 8, 2014

For the rest of the time, the horizontal power appears to be slightly larger, but by a much smaller amount. Also, there is a large departure from the mean power values sometime around June 28, which was likely caused by external interference.

5 Cross Polarization Power

NCAR developed an external calibration method for use on the S-Pol radar that utilizes ground clutter and solar scans. The unique feature of this method is that the ground clutter scans are based on the cross polarization scatter components, or the off-diagonal terms of the radar scattering matrix. This method takes advantage of the radar reciprocity principle that states that the cross polarization powers returned from either precipitation or clutter targets (i.e. transmit H, receive V – transmit V, receive H) are equal assuming that the transmitted powers are equal (Hubbert, 2003). This is based on the well understood principle of reciprocity (Tragl, 1990). See Figure 15 for a simple demonstration of the concept based on use of ground clutter for the targets.

Along with the clutter (or precipitation) cross polarization power scans, this method requires a solar scan. By combining the power ratios and the solar scan outputs, the system bias can be obtained as shown in the equation below adapted from Hubbert, 2003.

$$Zdr_{true} = Zdr_{meas} * \frac{CP_{xv}}{CP_{xh}} * (Sun)^2 \quad (5)$$

In this equation, "Sun" is the mean ratio of the V channel to the H channel noise powers observed during a scan of the solar disk.

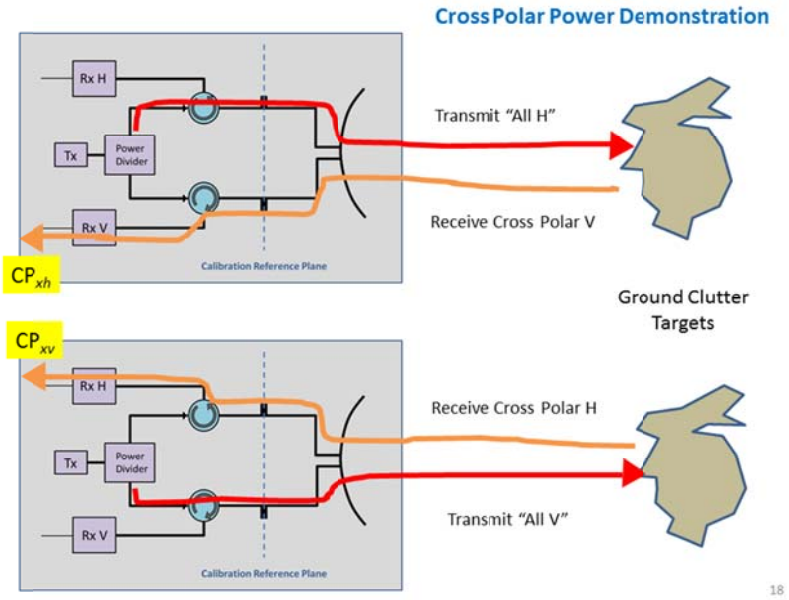

Figure 15: Cross Polar Power Demonstration

See Figure 16 for the terms needed to describe a simple proof of the cross polarization method. In Figure 13, all the relevant terms for comparing the intrinsic (or true) value for Z_{DR} to the measured Z_{DR} are indicated. These include all the hardware gains and losses and transmitter powers. This figure shows the origin of key parameters in the measured Z_{DR} and the cross polar powers of the equation above.

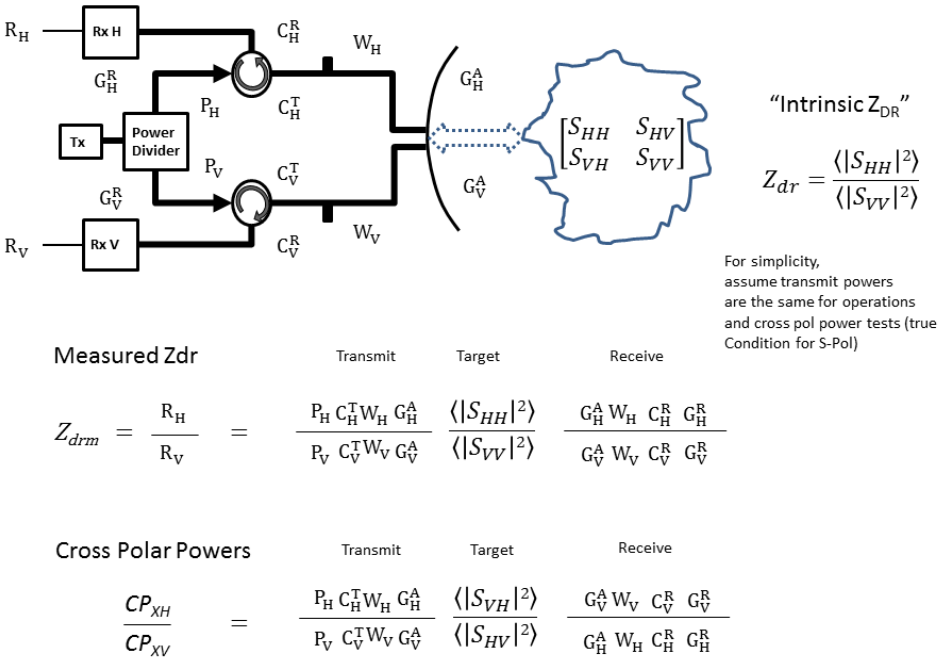

Figure 16: Cross Polar Power Relevant Terminology

Figure 17 is the algebraic demonstration of how the sun ratio and the cross polar power ratios combine to form the system bias. The "key to success" for this proof is that the sun ratio is defined as vertical noise to horizontal noise power, the inverse of convention. This key element results in the cancellation of almost all of the terms in the Zdr_{true} equation. The sun noise power ratios are assumed to be unity (the sun does not exhibit a polarization preference at microwave frequencies), and the cross polarization clutter power ratio is assumed to equal one via reciprocity.

The validity of the cross polarization power method has been extensively verified on the S-Pol radar (Hubbert, 2007a, 2011). NCAR first developed and verified the method using precipitation while operating the S-Pol radar in the so called "fast alternating" mode which uses a high speed rotary waveguide switch to alternately transmit the H and V pulses. This allowed the cross polar power pairs (CP_{XV}/CP_{XH}) to be obtained close together in time sequence. The NCAR team conducted vertical pointing calibrations in conjunction with the cross polarization power measurements and verified that the accuracies of the two methods are equivalent.

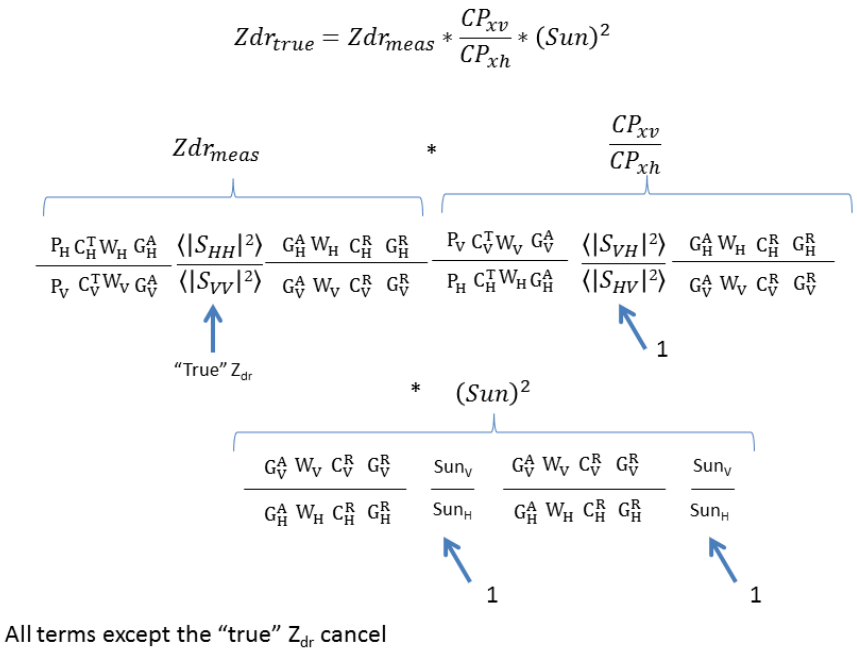

Figure 17: Algebraic Development of Cross Polar Power Concept

For application to the WSR-88D, NCAR modified the original cross polarization methods and collected data in what came to be called the "PPI Mode" for its similarity to the plan-position indicator type of scanning. This approach used alternating 360 degree scans, first one polarization, say H, followed by another scan using the alternate (or V) polarization. This meant that the H and V cross pol returns were not obtained as close in time as in the fast alternating mode. However, NCAR found that on the S-pol radar, the times were still sufficiently close to conclude that cross pol could yield the system Zdr bias values equivalent to the vertical pointing method.

Based on NCAR's results on S-pol, the ROC began implementation of the cross polarization power method on the WSR-88D. For evaluation purposes ROC software engineers modified the sun scan utility to generate the NCAR designed box scans and added utility code to control the radar in order to collect the sequential single polarization clutter powers. The following section describes the results from collecting cross polarization data on the test bed radars in Norman, Oklahoma (KCRI and KOUN).

In the course of implementing and testing the WSR-88D version of cross polarization power, the ROC and NCAR teams met several significant challenges. There were issues related to the cross polarization clutter power ratios, the solar scan derived reflector bias, and the transmitter power monitoring. The implementation issues are related to differences in the research radar (S-Pol) and the WSR-88D (Ice, 2013). The two radars have significant differences in antenna controls, transmitter power division, and receiver hardware. The WSR-88D antenna cannot be positioned and monitored to the same level of accuracy as the S-Pol antenna. The control characteristics of the WSR-88D pedestal present unique challenges for obtaining the clutter power ratios, essentially affecting the cross polar reciprocity assumption. This yields clutter power ratios with higher variances than those obtained with S-Pol (Ice, 2013). While S-Pol features a power division functionality that allows for the cross polar tests to be conducted at the same effective transmission power level used during operations, the WSR-88D features a variable phase power divider. This does not allow for the cross polar power testing to be done at the same power level as operations, and thus the ratios of the test and operational powers must be measured. This leads to complications, and increased error, that the engineering team must overcome (Meymaris, 2013).

7 The Lessons

The overall performance of the polarimetric WSR-88D with respect to Z_{DR} calibration is steadily improving through the efforts underway at the ROC. Sites that are having issues with calibration can be identified and assisted as needed through use of network wide monitoring tools becoming available. The use of the daily sunspike and emerging capabilities based on Bragg scatter as an external target show real promise in establishing and maintaining good Z_{DR} calibration.

The state of calibration for Z_{DR} is more mature at this point of deployment than reflectivity calibration was at a similar juncture in the early days of NEXRAD. Given the challenges summarized here, the fact that about 60% of the network sites are believed to be well calibrated is noteworthy. The network radars have been polarimetric for a bit over one year. The ROC continues to work with the field to identify and correct issues. The ROC science and engineering teams, supported by NCAR and NSSL, continue to develop tools for monitoring network performance. Following are discussions of specific functional areas where significant lessons resulted from the early deployment of the WSR-88D polarimetric upgrade.

7.1 Solar Scanning

The WSR-88D sun scan method for determining antenna pointing can occasionally produce erroneous results, especially if the scans are made in the presence of external interference, or if the hardware is not in good order. The simple method of scanning horizontally and vertically in a line as the sun passes can result in the fitted parabola not representing the true antenna reference position. Figure 18 is an example where instabilities in the position monitoring hardware, and the presence of external interference, caused poor fits of the parabola's to the azimuth and elevation noise power data. Were the results of this particular test to be used to correct antenna positioning data, significant errors in both the absolute antenna gain and the antenna differential channel bias would result.

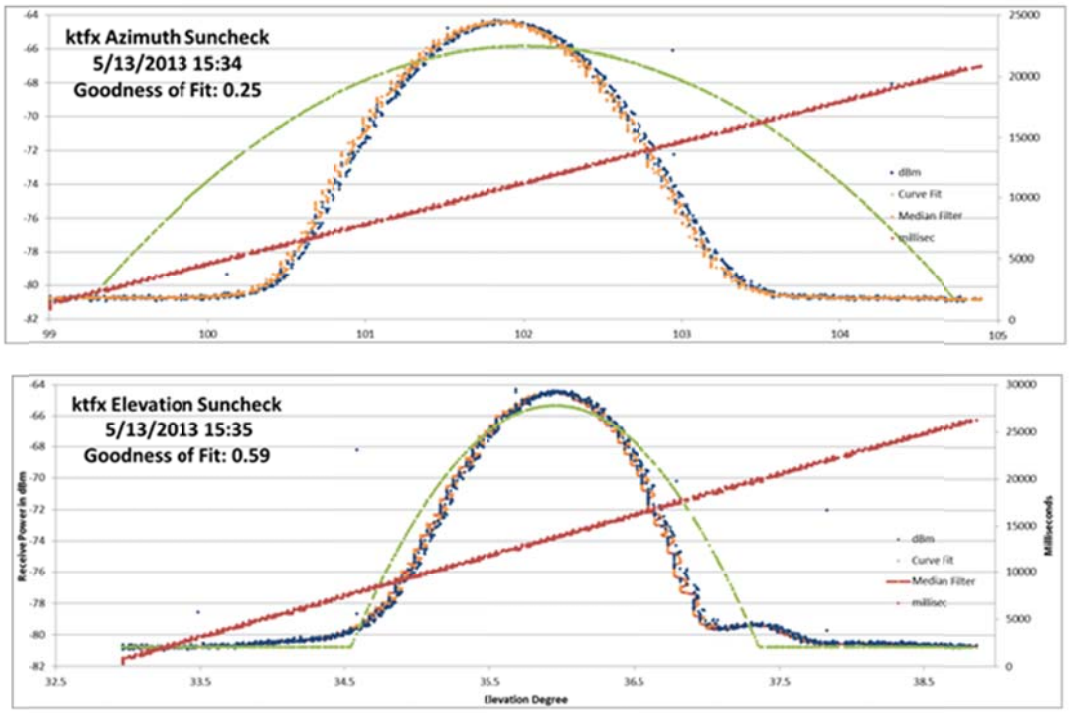

Figure 18: Example of a Failure in the Antenna Positioning Sun Scan Analysis

The ROC team is developing refinements to the solar scan process. As noted earlier, errors in positioning of the antenna can lead to incorrect values of antenna bias. The team is considering adapting the so "box scan" where the

antenna scans a relatively wide sector around predicted positions of the sun. These scans are then assembled into a two dimensional image as in Figure 19. Methods for conducting these types of scans, also called "scanning windows", are represented in the literature (Muth, 2012; Hubbert, 2011).

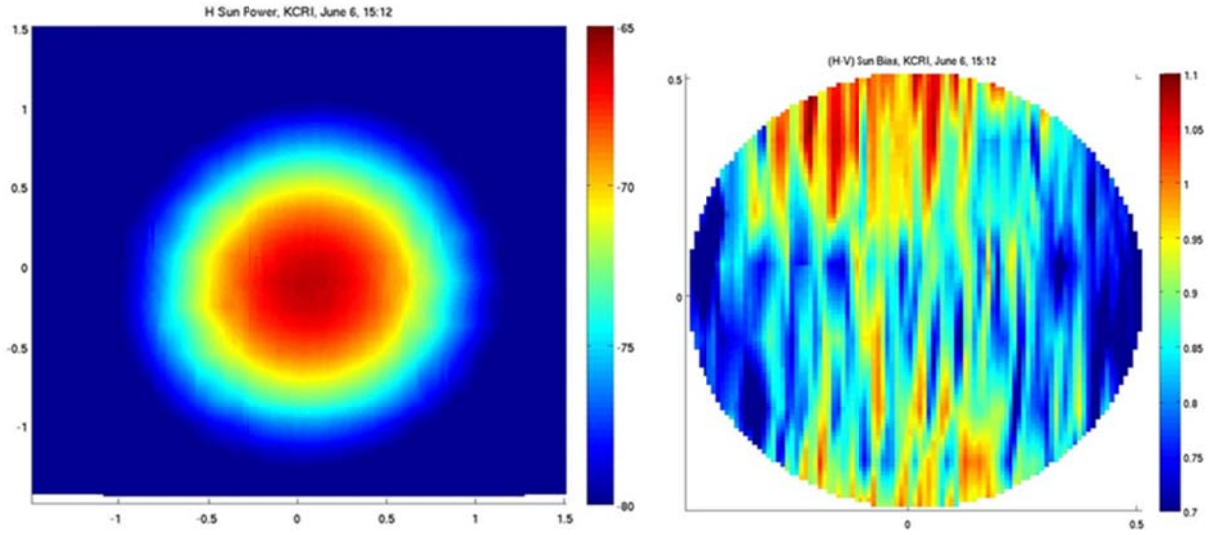

Figure 19: Two-Dimensional Image of Solar Noise Power and Sun Bias

One way to deal with antenna pointing errors and the resultant effect on the antenna bias component of calibration is to take advantage of a reliable external measurement. The daily sunrises and sunsets are excellent sources for monitoring antenna pointing (Holleman, 2010). The ROC technical team has implemented tools that search the radar data records, identifying and analyzing the daily sunspikes to infer not only the pointing accuracy, but also the Z_{DR} bias. This is possible because, as mentioned earlier, the sun is unpolarized and therefore has a mean Z_{DR} of zero, and the position of the sun can be predicted with a high degree of accuracy. The ROC tools compare the observed center of the sunspike with the expected center, and also compute the mean Z_{DR}. This data is accumulated for long periods of time and presented to analysts by means of two dimensional plots. Figure 20 presents two examples, one for a well aligned radar and one for a misaligned system. Each point on the plots represent a single estimate of the radar reported beam positon relative to the expected sunspike center (center of the plot) and the mean Z_{DR} in the sunspike, represented by the color.

In the plot on the left of Figure 20, the points representing the position error are more or less centered on zero. This indicates the mean error in pointing is small. The corresponding values for Z_{DR} are also near zero (-0.012 dB) as expected for the differential reflectivity of the solar noise signal. This represents a well calibrated system. The plot on the right shows a marked skewing of the position errors to the lower half of the plot, indicating that when the peak of the solar signal is found, the reported elevation position of the antenna is lower than the actual position. The mean value of the Z_{DR} estimates are strongly negative (-0.72 dB). Because the antenna control system "believes" the antenna is pointing lower (by about 0.3 degrees) than it actually is, when the antenna is commanded to point at the sun during the bias measurement, the beam is not centered on the solar disk and is in fact pointing too high.

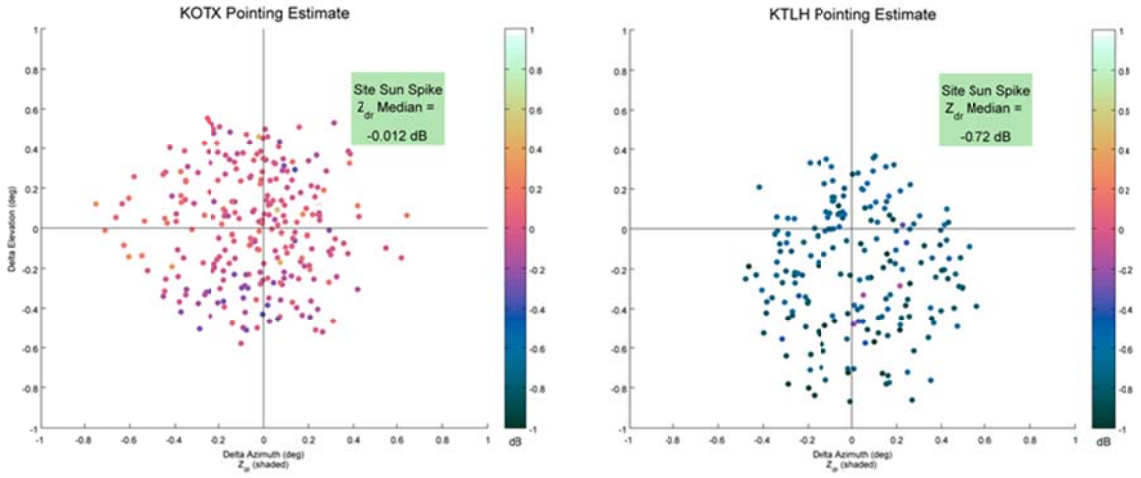

Figure 20: Sunspike Analysis of Antenna Pointing Error and Z_{DR} Bias for Spokane, WA (KOTX, left) and Tallahassee, FL (KTLH, right).

It is important to ensure that the beam is centered on the solar disk because the apparent angle subtended by the S-Band portion of the sun's emission spectrum is of the order of 30 minutes of arc, or 0.5 degrees, as seen in Figure 21, and this is comparable to the half power point beamwidth for the WSR-88D of less than one degree. In Figure 21, (adapted from Kundu, 1960 and Kennewell, 1989), the noise temperature for 3 GHz is relatively flat except for peaks at ±15 minutes of arc (subtended angle of 0.5 degrees). Then the noise temperature falls rapidly, extinguishing just inside the ±30 minutes of arc boundaries (one degree subtended angle). Even though the majority of the power exists within 0.5 degrees, there is some power beyond that limit. The non-linear nature of the sun noise temperature away from the center contributes to the uncertainty in bias measurements using the sun's emissions. Measurements taken when the antenna main lobe is not centered on the solar disk create asymmetrical conditions, resulting in unequal powers in the two orthogonal reception paths.

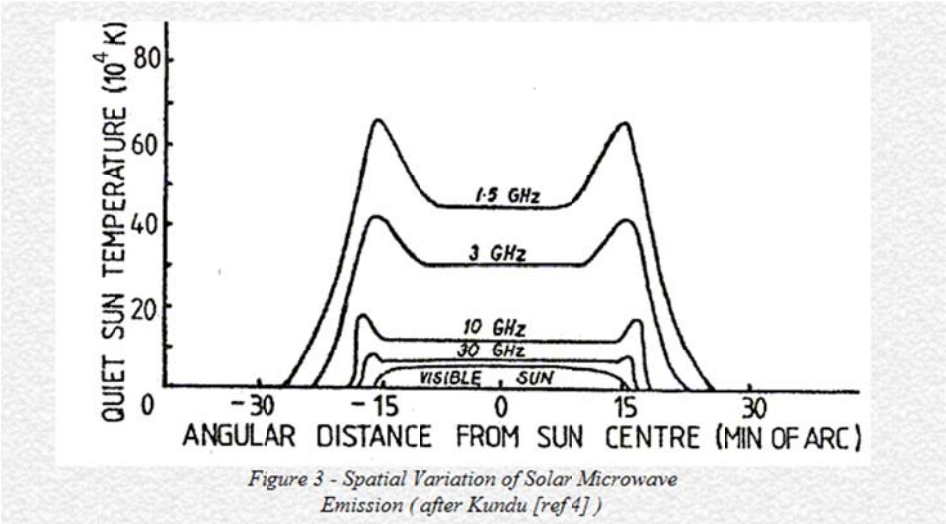

Figure 21: Sun Noise Temperature as a Function of Angular Distance from the Center of the Sun

From: http://www.spaceacademy.net.au/spacelink/solrfi/solrfi.htm with source citation of: Kundu MR, Solar Radio Astronomy, Wiley (New York), 1965

One final note regarding solar scanning is that it is important to conduct the sun scans with the conditions within the radar hardware established as close to operational as possible. As a specific example, the team discovered that the results of the solar scan antenna bias testing were dependent on whether the transmitter was operating or not. This was attributed to the temperature of the circulators, which were somewhat warmer when the transmitter was operating. As a result, all solar scans are obtained with the transmitter operating. This does lend some complication to the design of the solar scanning process and data collection to ensure returns from external targets do not contaminate the result. For example, clear air conditions are best and the sun scans are restricted to elevations above 10 degrees.

7.2 Hardware Measurements

The 30 dB test couplers located at the calibration reference plane are key components that have to be carefully characterized. As seen in equations 2 and 4, the loss factors for these couplers are components of the overall calibration determination. Uncertainties in these measurements translate directly into errors in the Z_{DR} bias measurement. The contractors that supplied the RF components believe the factory measurements are accurate within about 0.02 dB. However, examination of the plots in Figure 2 cast some doubt on this expectation. The variation of the measured loss factors varies by much more that 0.02 dB between adjacent points as the test equipment scanned over the frequency band in 5 MHz steps. The ROC team is investigating the uncertainty of this process and will conduct further testing on selected couplers. This investigation will include statistical analysis as part of an effort to reduce the variance of this data. An example of this type analysis is shown in Figure 2 where the green line represents a quadratic curve fit to the data. This curve is more representative of the theoretical performance of these Moreno Cross Guide couplers and is an attempt to smooth out the apparent instrumentation noise. In another example, the red dashed lines are plots of a 7-point moving average curve.

The ROC team plans to establish a rigorous test program for these couplers. The statistical analysis results will be compared to the new hardware tests conducted in the ROC Engineering Branch laboratory. The goal is to establish the accuracy of the statistical analysis through this comparison. If that succeeds, then the loss factors for all the fielded systems can be updated based on the statistics rather than requiring expensive and time consuming field tests.

7.3 Noise Estimation

Accurate measurement or estimation of the noise power in both channels is critical to maintaining acceptable bias levels in the Z_{DR} product. In fact, accurate handling of noise contamination is central to the production of high quality data. The community has focused significant effort on the measurement and removal of noise in polarimetric systems (Unal, 2012). There is some indication that precise noise measurements could serve as another indicator of receiver channel bias. The ROC team will explore this concept.

As seen in the example of Figure 14, issues with the hardware and external interference can result in noise measurements of dubious quality. Because the channel power estimates are corrected for the assumed noise powers, poor noise measurements can result in a bias in power ratios, or Z_{DR}, especially for low signal to noise ratios. In the WSR-88D baseline system, the noise is measured for both channels during the re-trace period at the end of each volume scan, with the measurement conducted at the highest elevation angle available. This is in order to obtain an estimate as close to “blue sky” conditions as possible. However, the noise powers are higher at lower elevations due to external features such as ground clutter and the estimates must be adjusted for lower elevations. This is done by means of an off-line test that scans the radar’s environment. The noise adjustment calibration itself can be corrupted by interference and a noisy local environment, resulting in various errors in the noise power estimates.

The solution to vulnerabilities in noise measurements is to infer the noise powers from the data itself, typically in a radial by radial basis. This has been done in the WSR-88D (Ivić, 2013). Figure 21 is an example of the H and V channel noise powers estimated on a per-radial basis. The upper two panels in Figure 21 depict the radially estimated noise power for both H and V channels as a function of azimuth. This is for the Tucson, Arizona, WSR-88D. The variation of the noise power of more than 1 dB from the baseline measured noise is due to the radar beam

scanning the mountains near Tucson. This demonstrates the clutter environment's effect on noise. The bottom panel displays the noise power difference between the channels and depicts a slight effect as the beam scans the mountains, demonstrating some polarization dependent noise components.

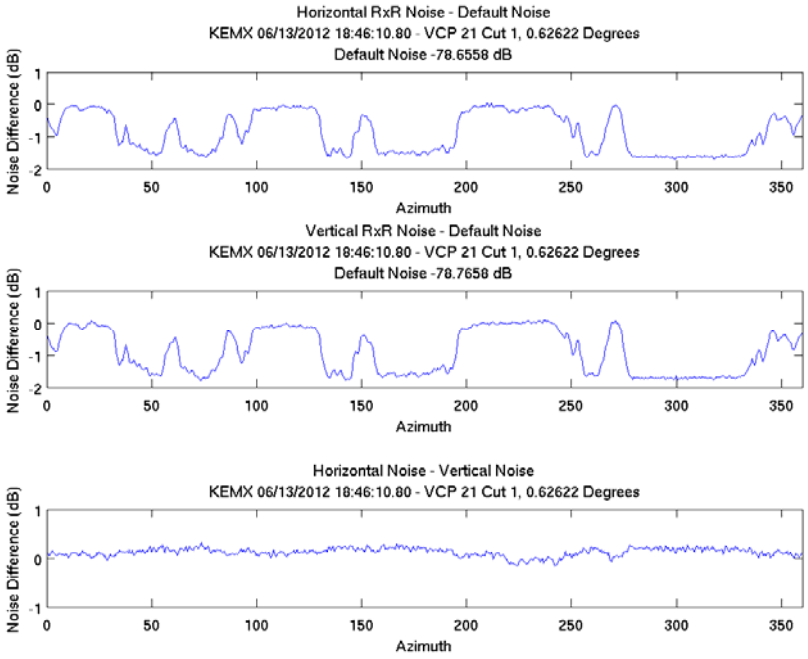

Figure 21: Noise Power Estimates on a Per-Radial Basis

7.4 External Target Measurements

The ROC team developed several methods for estimating the calibration state of the network radars. This work has been well described recently (Zittel, 2014; Hoban, 2014; Cunningham, 2013). These methods use hydrometeors (light rain and dry snow) and Bragg scatter. By using these methods, the ROC has determined that approximately 60% of the WSR-88D sites have external target derived bias estimates of within ±0. 2dB. Figure 22 is one example of an analysis product from the external target bias estimation process. It is a histogram of the bias estimates derived from analyzing returns from dry aggregated snow during the month of March 2014. This method is based on well characterized properties of dry snow (Ryzhkov, 2005, 1998). As Figure 22 shows, about 24 % of the sites have estimated bias values of less than 0.2 dB while 15 % have estimated bias values of greater than 0.2 dB.

At this time, the ROC team has not determined if the variance in the bias estimation histograms is due to the natural variation in the external target characteristics or due to some other related phenomena such as contamination by other types of scattering targets. The variance could also be showing the uncertainty of the engineering calibration measurements. If the histogram were viewed as following a Gaussian distribution, then the variance seems to be between 0.2 and 0.3 dB. As a reminder, the NCAR studies concluded that engineering type calibrations were expected to exhibit an uncertainty of about 0.25 dB, and the network performance seems to fit that expectation. The observed results are likely due to a combination of the uncertainty of the external methods and the uncertainty of the engineering calibrations.

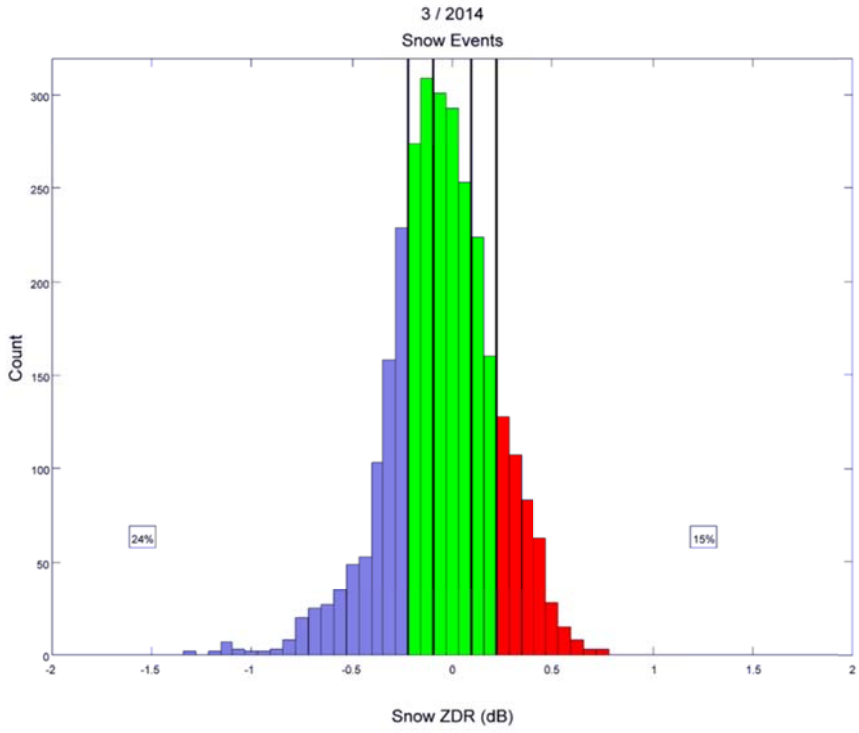

7.5 Cross Polar Power

Cross polar power continues to be a potentially attainable true external calibration technique that could rival the vertical pointing method. This will be the case if the ROC and NCAR teams can surmount the challenges presented by the WSR-88D design. The serious challenges to date derive from major differences in the hardware design of the S-Pol radar, where the cross pol method was developed, and the WSR-88D. The major differences are in the pedestal control and transmit power division. Some other differences which could account for the performance challenge are the antenna design and the location of the low noise amplifiers.

The S-Pol radar features a robustly designed antenna that is not enclosed in a radome and is much more mechanically rigid than the WSR-88D antenna. The radome itself may be contributing to the observed performance issues. Members of the meteorological radar community have investigated the effects of the radome on differential power measurements (Frech, 2013, 2011; Gorgucci, 2013). The S-Pol low noise amplifiers are located in a climate controlled shelter while the WSR-88D amplifiers are in the RF Pallet, housed in the radome. However, the WSR-88D amplifiers are provided with internal temperature compensation. It remains to be seen if the temperature performance differences are an issue. Also, there are some early indications that there is a slight mismatch in linearity between the H and V receivers in the WSR-88D that could affect Z_{DR} accuracy (Melnikov, 2013b).

8.0 Summary and Recommendations

All of these items highlight the challenges of migrating research capabilities into operational radar networks. During the extended research phase for polarimetric weather radar spanning the 1970's to the 21st Century, scientists and engineers focused much effort on the calibration problem. In most cases, satisfactory results required use of an external method, most commonly the vertical pointing and scanning method described by Gorgucci in 1999 and Bringi and Chandra (Bringi and Chandrasekar, 2001). What works well in a research environment may not be easily adapted to production systems. When planning new field capabilities based on scientific research, engineers need to be cognizant of the differences between research platforms and the target field systems. This can be dealt with

through careful planning for all Research-to-Operations (R2O) processes. The lessons learned in this project and other recent enhancements are being applied to future work.

It is apparent from the US NEXRAD program efforts, and from reports of others in the community, that a multi-faceted, comprehensive, and centrally managed approach is needed in order to achieve the remarkably stringent requirements for differential reflectivity calibration for operational networks. In recent years, other national network operators and researchers have reported on their efforts to implement continuous data quality projects (Frech, 2013; Figueras I Ventura, 2012; Gourley, 2006). These all use combinations of equipment measurements and continuous monitoring with external targets. Technical investigators around the community should continue to consider ever more creative ways to calibrate their radar networks, perhaps leveraging the increasing knowledge base of microphysical parameter behavior. One example is the proposed use of observed deviations in the expected vertical profile of differential reflectivity as a bias indictor (Bechini, 2008), again an external target method. Other types of external targets have been proposed. The use of metal calibration spheres, either tethered (Williams, 2013) or free floating (Pratte, 2005; Ice, 2005), has been proposed and some testing has been done. Bouncing the radar signal off of the lunar surface has also been investigated (Melnikov, 2013b; Pratte, 2005). As it turns out, measurable returns from the moon can be obtained with S-Band weather radars.

The lessons learned from the past ten years of investigation and testing can be summarized in a set of rules that may be helpful for those contemplating the design and development of new polarimetric radars. The rules are:

1. Consider calibration in all aspects of requirements development and design for calibration.
2. Polarimetric weather radars should be as simple as possible, but not simpler (to paraphrase Dr. Einstein).
3. Monitor all system parameters continuously
4. Check the "Checker"…or, monitor your built-in-test equipment carefully.
5. Create an error budget, and be aware of the effect of each component on the budget.
6. Employ multiple measurements, external as well as internal.
7. Get help! Make sure to consider the community's experiences.
8. Calibrate how you operate.
9. Treat calibration as a network problem, compare radar performances across the fleet.
10. Question everything, especially manufacturer's data.

The ROC team continues to develop better methods of engineering calibration coupled with increased use of external methods for evaluating the state of each network radar's calibration. The ROC will develop four distinct projects aimed at improving calibration. The first efforts are focusing on the test software that supports calibration. The engineering teams are simplifying procedures and automating some tasks to reduce errors. The second project is developing the external target monitoring methods, i.e. migrating the research capability to an operational mode. This will allow personnel in the field as well as network managers to assess the performance of each radar in near-real time. The third project is for engineering investigations into the hardware, and includes the goal of reducing the uncertainty of the coupler loss measurements. Eventually the fourth project will focus on using external target measurements to adjust the base differential reflectivity estimates.

It's clear that attaining the goal of reducing the uncertainty of Z_{DR} estimates to below 0.1 dB will not be solved by any one, or by any few, methods. It requires a holistic approach, leveraging advances in engineering with novel uses

of external targets. The ROC team plans to continue to address the issue of calibration with a number of diverse efforts to ensure the quality of NEXRAD polarimetric data is as good as it can be.

Acknowledgments

The authors wish to express appreciation to Dr. John Hubbert, Dr. Greg Meymaris and Dr. Mike Dixon of NCAR for their technical support to the cross polarization power calibration project, and to Dr. Valery Melnikov of NSSL for his excellent analysis of the current calibration methods. We also wish to thank Mr. Mike Istok of the National Weather Service Office of Science and Technology for providing vital support to the NSSL team.

References

Balaji, M. S., J. R. Ellis, W. H. Walker, D. R. Cartwright, J. H. Lee, J. H. Romines, 2012, An Engineering Illustration of the Dual Polarization upgrade for the WSR-88D, ERAD 2012, *7th European Conference on Radar in Meteorology and Hydrology.*

Baron Services, 2011, ZDR Calibration Accuracy Analysis, BS-2000-000-107, Available from Baron Services Inc. 4930 Research Dr., Huntsville Alabama, 35805 USA

Bechini, R., L. Baldini, R. Cremonini and E. Gorgucci, 2008, Differential Reflectivity Calibration for Operational Radars, *J. Atmos. Oceanic Technol.*, **25**, 1542 - 1555.

Berkowitz, D. S., J. A. Schultz, S. Vasiloff, K. L. Elmore, C. D. Payne, and J. B. Boettcher, 2013, Status of Dual Pol QPE in the WSR-88D Network, *27th Conference on Hydrology.*

Bringi, V. N., T. Seliga and S. M. Cherry, 1983, Statistical Properties of the Dual Polarization Differential Reflectivity (ZDR) Radar Signal, *IEEE Trans. On Geoscience and Remote Sensing*, **GE-21**, No 2, Apr 1983, 215 - 220.

Bringi, V. N., V. Chandrasekar, P. Meischner, J. Hubbert and Y. Golestani, 1991, Polarimetric Radar Signatures of Precipitation at S- and C-bands, *IEEE Proceedings-F*, **138**, No. 2, April 1991, 109 – 119.

Bringi, V. N. and Chandrasekar, V., 2001, Polarimetric Doppler Weather Radar, Cambridge University Press.

Brunkow, D., V. N. Bringi, P. C. Kennedy, S. A. Rutledge, V. Chandrasekar, E. A. Mueller and R. K. Bowie, 2000, A Description of the CSU-CHILL National Radar Facility, *J. Atmos Oceanic Technol.,* **17**, 1596 - 1608.

Cao, Q, G. Zhang, E. Brandes, T. Schuur, A. Ryzhkov and K. Ikeda, 2008, Analysis of Disdrometer and Polarimetric Radar Data to Characterize Rain Microphysics in Oklahoma, *J. App. Meteorology*, **47**, 2238 – 2255.

Cunningham, J. G., W. D. Zittel, R. R. Lee, R. L. Ice and N. P. Hoban, 2013, Methods for Identifying Systematic Differential Reflectivity (Zdr) Biases on the Operational WSR-88D Network, *36th Conference on Radar Meteorology.*

Figueras I Ventura, J., A. Boumahmoud, B. Fradon, P. Dupuy and P. Tabary, 2012, Long-term Monitoring of French Poarimetric Radar Data Quality and Evaluation of Several Polarimetric Quantitative Precipitation Estimators in Ideal Conditions for Operational Implementation at C-Band, *Q. J. R. Meteorol. Soc.* 2212 – 2228, October 2012.

Free, A. D., N. K. Patel, R. L. Ice and O. E. Boydstun, 2007, WSR-88D ORDA Antenna Gain and Beamwidth Algorithms, *23rd International Conference on Interactive Information Processing Systems for Meteorology, Oceanography, and Hydrology.*

Frech M., B. Lange, T. Mammen, J. Seltmann, C. Morehead and J. Rowan, 2013, Influence of a Radome on Antenna Performance, *J. Atmos Oceanic Technol.,* **30**, 313-324.

Frech, M., 2013, Monitoring the Data Quality of the New Polarimetric Weather Radar Network of the German Meteorological Service, *36th Conference on Radar Meteorology.*

Frech, M., B. Lange, T. Mammen, J. Seltmann, C. Morehead and J. Rowan, 2011, Onsite Radome Performance Verification, *35th Conference on Radar Meteorology.*

Gorgucci, E., R. Bechini, L. Baldini, R. Cremonini and V. Chandrasekar, 2013, The Influence of Antenna Radome on Weather Radar Calibration and Its Real Time Assessment, *J. Atmos Oceanic Technol.,* **30**, 676-689.

Gorgucci, E, S. Gianfranco, and V. Chandrasekar, 1999, A Procedure to Calibrate Multiparameter Weather Radar Using Properties of the Rain Medium, *IEEE Trans. On Geoscience and Remote Sensing*, Vol. 37, No 1, Jan 1999.

Gourley, J. J., B. Kaney, and R. A. Maddox, 2003, Evaluating the Calibrations of Radars: A Software Approach, *31st Conference on Radar Meteorology.*

Gourley, J. J., P. Tabary and J. Parent du Chatelet, 2006, data Quality of the Meteo-France C-Band Polarimetric Radar, *J. Atmos. Oceanic Technol.*, **23**, 6961340 - 1356.

Hoban, Nicole P., J. G. Cunningham and W. D. Zittel, 2014, Estimating Systematic WSR-88D Differential Reflectivity (Z_{DR}) Biases Using Bragg Scattering, *30th Conference on Environmental Information Processing Technology.*

Holleman, I, A. Huuskonen, R. Gill, P. Tabary, 2010: Operational Monitoring of Radar Differential Reflectivity Using the Sun. *J. Atmos Oceanic Technol.,* **27**, 881-887.

Hubbert, J. C., V. N. Bringi, and D. Brunkow, 2003, Studies of the Polarimetric Covariance Matrix. Part I: Calibration Methodology, *J. Atmos. Oceanic Technol.*, **20**, 696 - 706.

Hubbert, J. C., F. Pratte, M. Dixon, R. Rilling, and S. Ellis, 2007a, Calibration of Zdr for NEXRAD, *23rd International Conference on Interactive Information Processing Systems for Meteorology, Oceanography, and Hydrology.*

Hubbert, J. C., F. Pratte, M. Dixon and R. Rilling, 2007b, The Uncertainty of Zdr Calibration Techniques, *33rd Conference on Radar Meteorology.*

Hubbert, J. C., F. Pratte, M. Dixon and R. Rilling, 2008, NEXRAD Differential Reflectivity Calibration, *24th International Conference on Interactive Information Processing Systems for Meteorology, Oceanography, and Hydrology.*

Hubbert, J. C., Dixon, M., Chandrasekar, V.,Brunkow, D. A., Kennedy, P. C., Ice, R. L., Heck, A. and Saxion, D., 2011, Zdr Calibration and Simultaneous Horizontal and Vertical Transmit Operation, *35th Conference on Radar Meteorology.*

Hubbert, J. C., M. Dixon, R. Ice, D. Saxion and A. Heck, 2012, Differential Reflectivity Calibration for Simultaneous Horizontal and Vertical Transmit Radars, *7th European Conference on Radar in Meteorology and Hydrology.*

Huuskonen, A. and I. Holleman, 2007, Determining Weather Radar Pointing Using Signal Detected from the Sun at Low Antenna Elevations, *J. Atmos. Oceanic Technol.*, **24**, 426 - 483.

Ice, R. L., D. A. Warde, F. Pratte, 2005, Investigating External and Dual Polarization Calibration Options for the WSR-88D, *32nd Conference on Radar Meteorology.*

Ice, R. L., R. D. Rhoton, J. C. Krause, D. S. Saxion, O. E. Boydstun, A. K. Heck, J. N. Chrisman, D. S. Berkowitz, W. D. Zittel, and D. A. Warde, 2009, Automatic Clutter Mitigation in the WSR-88D, Design, Evaluation, and Implementation, *34th Conference on Radar Meteorology.*

Ice, R. L., J. G. Cunningham and A. K. Heck, 2013, Polarimetric Weather Radar Calibration – Engineering Challenges, *36th Conference on Radar Meteorology.*

Illingworth, A. J. and I. J. Taylor, 1989, Polarization Radar Estimates of Raindrop Size Spectra and Rainfall Rates, *J. Atmos. Oceanic Technol.*, **6**, 939 - 949.

Ivić Igor R., C. Curtis and S. Torres, 2013, Radial-Based Noise Power Estimation for Weather Radars, *J.* Atmos. *Oceanic Technol.*, **30**, 2737 – 2753.

Kennewell, J. A., 1989, Solar Radio Interference to Satellite Downlinks, *6th International Conference on Antennas and Propagation IEEE ICAP89*, 334 – 339.

Kundu, M. R., 1965, Solar Radio Astronomy (Wiley, N. Y.)

Melnikov, V., R. J. Doviak, D. S. Zrnić and D. J. Stensrud, 2013a, Structures of Bragg Scatter Observed with the Polarimetric WSR-88D, *J. Atmos. Oceanic Technol.*, **30**, 1253 - 1258.

Melnikov, V. and D. Zrnić, 2013b, Calibrating Differential Reflectivity in the WSR-88D, National Severe Storms Laboratory (http://www.nssl.noaa.gov/publications/wsr88d_reports/WSR88D_ZDRcalib_Report_2013.pdf).

Melnikov, V. M, R. J. Doviak, D. S. Zrnić and D. J. Stensrud, 2011, Mapping Bragg Scatter with a Polarimetric WSR-88D, *J. Atmos. Oceanic Technol.*, **28**, 1273 - 1285.

Meymaris, G, J. C. Hubbert, M. Dixon, R. L. Ice and A. K. Heck, 2013, Operational Considerations for Zdr Calibration Using the Cross-Polarimetric Technique, *36th Conference on Radar Meteorology.*

Muth, X., M. Schneebeli and A. Berne, 2012, A Sun-tracking Method to Improve the Pointing Accuracy of Weather Radar, *Atmos. Meas. Tech.*, **5**, 547 – 555.

Pratte, F. and R. L. Ice, 2005, External Radar Calibration Options Applicable to the WSR-88D Network, Radar Operations Center (ROC) Report, April 18, 2005, available from the ROC.

Ryzhkov, A. V. et al, 2005, Calibration Issues of Dual-Polarization Radar Measurements, *J. Atmos. Oceanic Technol.*, **22**, 1138 - 1155.

Ryzhkov, A. V. and D. Zrnić, 1998, Discrimination between Rain and Snow with a Polarimetric Radar, *J. App. Meteorology*, **37**, 1228 – 1240.

Saxion, D. S. and R. L. Ice, New Science for the WSR-88D: Status of the Dual Polarization Upgrade, 2012, *28th International Conference on Interactive Information Processing Systems for Meteorology, Oceanography, and Hydrology.*

Seliga, T. A. and V. N. Bringi, 1976, Potential Use of Radar Differential Reflectivity Measurements at Orthogonal Polarizations for Measuring Precipitation, *J. App. Meteorology*, **15**, 69 – 76.

Sirmans, D., 1992, Calibration of the WSR-88D, Operational Support Facility Report, Available from the WSR-88D Radar Operations Center.

Sirmans, D., D. Zrnić and M. Sachidananda, 1984, Doppler Radar Dual Polarization Considerations for NEXRAD, National Severe Storms Laboratory Draft Report for the Joint Systems Project Office, (available from the WSR-88D Radar Operations Center).

Smith, P. L, The Unit Symbol for the Logarithmic Scale of Radar Reflectivity Factors, 2010, *J. Atmos. Oceanic Technol.*, **27**, 615 – 616.

Tragl, K., 1990, Polarimetric Radar Backscattering from Reciprocal Random Targets, *IEEE Trans. Geosci. Remote Sens.*, **28** No. 5, 856 – 864.

Unal, C., Y. Dufournet, T. Otto and H. Russchenberg, 2012, The New Real-time Measurement Capabilities of the Profiling TARA Radar, *7th European Conference on Radar in Meteorology and Hydrology.*

Williams, E, K. Hood, D. Smalley, M. Donavan, V. Melnikov, D. Forsyth, D. Zrnić, D. Burgess, M. Douglas, J. Sandifer, D. Saxion, O. Boydstun, A. Heck and T. Webster, 2013, End-to-end Calibration of NEXRAD Differential Reflectivity with Metal Spheres, *36th Conference on Radar Meteorology.*

Zittel, W. D., J. G. Cunningham, R. R. Lee, L. M. Richardson, R. L. Ice and V. Melnikov, 2014, Use of Hydrometeors, Bragg Scatter, and Sun Spikes to Determine System Z_{DR} Biases in the WSR-88D Fleet, *8th European Conference on Radar in Meteorology and Hydrology.*

Zrnić, D. S., R. Doviak, G. Zhang and A. Ryzhkov, 2010, Bias in Differential Reflectivity Due to Cross Coupling Through the Radiation Patterns of Polarimetric Weather Radars, *J. Atmos. Oceanic Technol.*, **27**, 1624 - 1637.

Zrnić, D. S., Melnikov, V. M. and J. K. Carter, 2006, Calibrating Differential Reflectivity on the WSR-88D, *J. Atmos. Oceanic Technol.*, **23**, 944 - 951.